A Hybrid Biomonitoring System for Gut-Neuron Communication

Ashley A. Chapin, Jinjing Han, Ta-Wen Ho, Jens Herberholz, and Reza Ghodssi, *Fellow, IEEE*

***Abstract*— This work presents an integrated electrochemical and electrophysiological biomonitoring system, enabling the study of molecular signaling along the gut-brain-axis (GBA). *In vitro* gut cell cultures provide a controllable, accessible platform to study gut physiology. Similarly, the *ex vivo* crayfish abdominal nerve cord provides a model for the electrophysiological study of nerve signaling. For the first time, our system integrates these platforms to enable the study of signaling from gut to nervous system, which *in vivo* would influence the brain. The platform consists of two interconnected modules: (I) the electrochemistry module (ECM), mimicking a Transwell platform for cell growth and enabling neurotransmitter (serotonin (5-HT)) detection, and (II) the electrophysiology module (EPM), hosting a dissected crayfish nerve cord and allowing electrode accessibility for the assessment of nerve responses to 5-HT. Whole system integration is aided by the inclusion of a flexible heater to maintain cells near body temperature (38° C), transwell membrane modification to improve molecular diffusion (450-fold) while maintaining good cell compatibility, and precise flow-controlled 5-HT transport from ECM to EPM. This work achieves module-specific environmental control, which will ultimately enable the study of molecular signaling between gut and nerve cells to facilitate real-time monitoring of both tissues within the GBA. [2020-0151]**

***Index Terms*— Biological systems, biomedical transducers, electrochemical devices, electrophysiology, fluidic microsystems.**

Manuscript received May 11, 2020; revised May 27, 2020; accepted May 28, 2020. Date of publication June 23, 2020; date of current version October 7, 2020. This work was supported in part by the National Science Foundation Neural and Cognitive Science Program under Award 1926793, in part by the University of Maryland Nanocenter and its FabLab, and in part by the Terrapin Works Advanced Fabrication Lab Facilities. Subject Editor R. Sochol. *(Corresponding author: Reza Ghodssi.)*

Ashley A. Chapin is with the Fischell Department of Bioengineering, University of Maryland, College Park, MD 20742 USA, also with the Fischell Institute for Biomedical Devices, University of Maryland, College Park, MD 20742 USA, and also with the Institute for Systems Research, University of Maryland, College Park, MD 20742 USA (e-mail: aachapin@umd.edu).

Jinjing Han is with the Department of Electrical and Computer Engineering, University of Maryland, College Park, MD 20742 USA, and also with the Institute for Systems Research, University of Maryland, College Park, MD 20742 USA (e-mail: jhan977@umd.edu).

Ta-Wen Ho and Jens Herberholz are with the Department of Psychology, University of Maryland, College Park, MD 20742 USA, and also with the Neuroscience and Cognitive Science Program, University of Maryland, College Park, MD 20742 USA (e-mail: twho@umd.edu; jherberh@umd.edu).

Reza Ghodssi is with the Fischell Department of Bioengineering, University of Maryland, College Park, MD 20742 USA, also with the Fischell Institute for Biomedical Devices, University of Maryland, College Park, MD 20742 USA, also with the Department of Electrical and Computer Engineering, University of Maryland, College Park, MD 20742 USA, and also with the Institute for Systems Research, University of Maryland, College Park, MD 20742 USA (e-mail: ghodssi@umd.edu).

Color versions of one or more of the figures in this article are available online at http://ieeexplore.ieee.org.

Digital Object Identifier 10.1109/JMEMS.2020.3000392

I. Introduction

A. Gut-Brain-Axis (GBA)

THE gut-brain-axis (GBA) is a bidirectional signaling pathway between the gastrointestinal (GI) tract, the enteric nervous system, and the brain. Environmental and chemical factors in the gut can affect mood and behavior [1], and dysregulation of the GBA pathway can have a significant impact on GI and neurological disorder development [2]. The neurotransmitter serotonin (5-HT) is a major signaling molecule in the gut and is also known to stimulate the vagus nerve to regulate neural processes [3]. Enterochromaffin cells within the GI epithelium are the main producers of 5-HT; they sense luminal conditions and undergo secretory granule release of 5-HT on their basolateral side to stimulate local peripheral nerves [4]. Current understanding of the GBA mostly comes from studies in animal models, in which the addition of certain food or gut bacteria have been shown to affect hormone levels, behavior, and brain development [2] [5], [6]. However, it is difficult to study how the release of 5-HT and downstream nervous activation are affected by these luminal stimuli. Current technology is unable to directly monitor 5-HT signaling at the interface between gut cell cultures and nervous tissue. Real-time monitoring would allow researchers to investigate the effects of environmental stimuli on 5-HT release dynamics and subsequent nerve activation. 5-HT can be detected electrochemically, and serotonergic neuronal activation can be monitored electrophysiologically, but this has not yet been achieved in a single system.

B. Crayfish as a Model Organism for Electrophysiology and Neuropharmacology

The crayfish is a classical, well established invertebrate model for electrophysiology, which measures electrical impulses caused by changes in neuron membrane potentials in response to a sensory stimulus [7]. The crayfish abdominal nerve cord contains a pair of lateral giant (LG) interneurons with large, accessible axons that communicate sensory inputs to the motor systems for stimulating escape behavior in response to predatory attacks [8]. This allows extra- and intracellular electrode placement to stimulate and record activity in a neural circuit. In addition, the nerve cord is connected to the gut, and bidirectional communication is mediated via serotonergic fibers and ascending interneurons, similar to the mammalian vagus nerve, making it a promising model to investigate serotonin-mediated pathways from gut to brain.

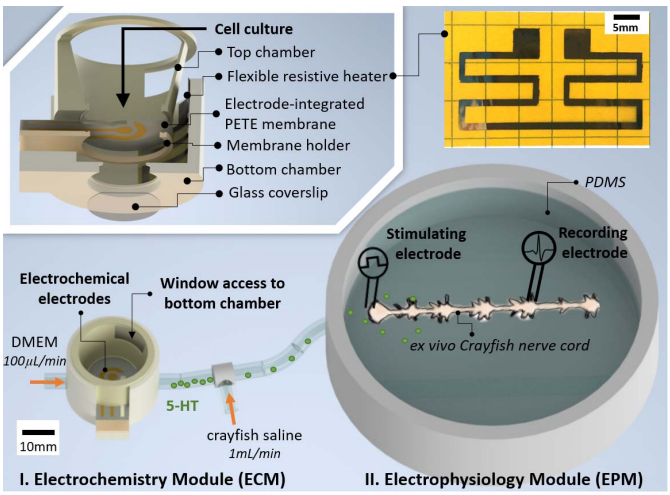

Fig. 1. ECM and EPM full system integration. Inset, left: Exploded view of ECM components. Inset, right: AU Heater patterned on polyimide substrate.

C. Integration of Gut and Neuron Monitoring Systems

Despite the interest in real-time monitoring of nervous signaling from gut to brain, no work thus far has aimed to leverage the existing tissue model systems of *in vitro* gut cultures and nerve cord electrophysiology. There are challenges associated with the combination of these platforms. Mammalian live cell assays require maintaining cells at body temperature (∼37°C) in an appropriate cell media and a sterilized, leak-proof container for protection against contamination. Crayfish nerve cord electrophysiology experiments are best performed at room temperature (RT, ∼25°C) in a dedicated crayfish saline solution, with access for electrode placement, and with mechanical stabilization and limited electrical noise.

Here, we report the development of a platform which integrates two recording modules for gut and nervous tissue. The electrochemistry module (ECM) allows for the growth of mammalian gut cell cultures on an electrochemical electrode-integrated porous membrane for *in situ* measurement of 5-HT using cyclic voltammetry (CV) and chronoamperometry (CA). The electrophysiology module (EPM) contains a dissected crayfish nerve cord and allows the placement of extra- and intra-cellular electrodes to measure modulation of neuronal activity in response to 5-HT injection in the ECM. A fluidic connection between the modules allows the ECM to be filled with cell media (DMEM), diluted with crayfish saline, and transported to the EPM to evaluate the effect of injected 5-HT – or in future work, cell released 5-HT – on nerve activity.

The ECM, diagrammed in Fig. 1 inset, was designed to resemble a transwell insert for *in vitro* cell culture. Cells can be grown on a 0.4 μm pore-diameter polyester track-etched (PETE) membrane suspended between a top and bottom chamber for apical and basolateral access. As previously reported [9], a carbon nanotube (CNT)-modified Au electrochemical sensor was patterned on the bottom side of the PETE membrane to detect 5-HT locally at the basolateral surface, which thus far has been demonstrated with controlled injections of 5-HT at known concentrations. This 0.4 μm PETE membrane supports excellent cell adhesion and monolayer formation, as opposed to membranes with larger pore diameters. However, diffusion is severely limited across this membrane, limiting the time resolution of detection of released or injected molecules. The rate of molecular diffusion across this membrane was enhanced by laser cutting holes (∼120 μm diameter) within or surrounding the working electrode (WE), increasing the time resolution and sensitivity to injected 5-HT. Finally, the ECM was fitted with a flexible resistive heater to maintain the internal solution temperature near 37°C during extended electrophysiology experiments at RT.

The EPM, diagrammed in Fig. 1, enables the dynamic electrophysiological recording of neural responses to 5-HT release events within the ECM. Its design is directly based on standard glass petri dish holders traditionally used for crayfish nerve cord electrophysiology, allowing perfusion of contents from the ECM chamber (i.e. crayfish saline diluted DMEM). The chamber was then filled with a layer of polydimethylsiloxane (PDMS), allowing a dissected crayfish nerve cord to be pinned inside the dish. The chamber was left open to allow access for electrode placement on the abdominal nerve cord and sensory nerves to stimulate and record the nerve cord response to injected stimulants (5-HT) transported from the ECM. Extracellular recording was used to detect LG action potentials while intracellular recording was used to detect excitatory postsynaptic potentials (EPSPs), which are subthreshold changes below activation of an action potential. A T-junction was used to dilute the DMEM with crayfish saline before perfusion into the EPM. The dilution factor was controlled by the ratio of the two flow rates. The fluidic connection allows mammalian cells to be maintained in DMEM while the crayfish nerve cord is exposed only to DMEM diluted with saline to minimize the effect of DMEM contents (e.g. tryptophan, glycine, glucose) on nerve activity.

The results reported here illustrate the individual functions of each module of the system, as well as a proof-of-concept protocol to assess 5-HT transport from the ECM to the EPM and serotonergic modulation of the crayfish LG.

II. Materials and Methods

A. Design and Fabrication of Modules

The **EPM** consists of a modified 100 mm diameter polystyrene petri dish with a 3/16-inch hole drilled on the side wall for fluidic tube insertion. 30 g of uncured PDMS was poured into the EPM and cured at 60°C for 3 hours to form the base of the dish. The **ECM** was designed similarly to a 12-well plate transwell insert, with a 15 mm diameter cell growth area on a PETE membrane separating a ∼3 mL volume bottom chamber and a ∼2 mL volume top chamber. Pipetting into the bottom chamber was enabled through a 6 mm-tall window in the top chamber wall (Fig. 1 inset). These pieces were 3D printed with an Objet Connex3 PolyJet printer (Stratasys) using MED610, a biocompatible resin. Support material was removed and MED610 pieces were thoroughly cleaned using a sonication protocol developed by Ngan *et al.* [10].

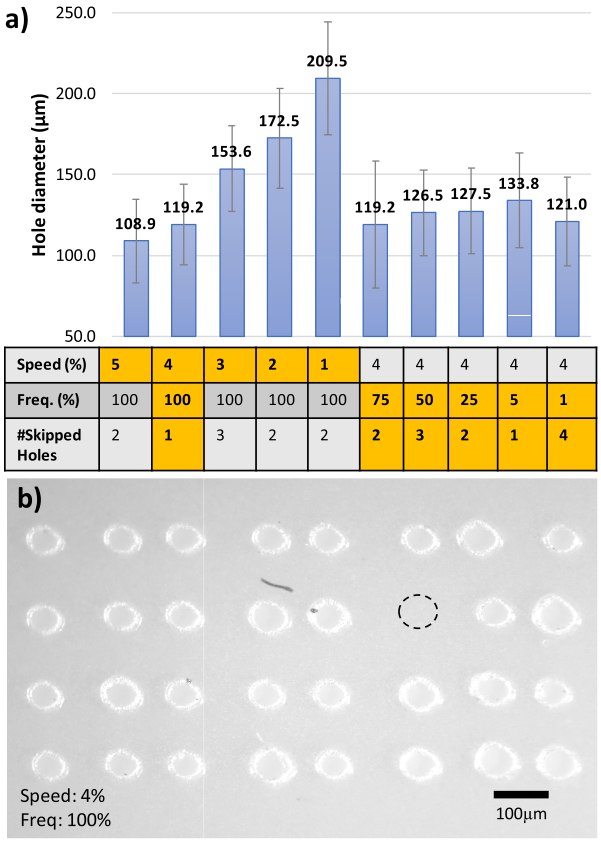

Speed (%)	5	4	3	2	1	4	4	4	4	4
Freq. (%)	100	100	100	100	100	75	50	25	5	1
#Skipped Holes	2	1	3	2	2	2	3	2	1	4

Fig. 2. Laser cut parameter optimization for modifying PETE membranes with patterned holes. (a) Plot of average diameter of laser cut holes corresponding to a variety of settings: Power 1%, Speed 1-5%, Frequency 1-100%. The number of skipped holes per 32-hole grid is labelled. (b) Image of laser cut hole grid pattern using optimized settings: Speed 4%, Frequency 100%, Power 1%. A skipped hole is marked with a dashed circle.

B. Modification of PETE Transwell Membranes

PETE membranes with 0.4 μm pores were purchased from Sterlitech, then laser cut to a 17 mm diameter using the Epilog Fusion M2 laser cutter (Epilog Laser). Some membranes were patterned with a grid of 34 laser cut holes (0.5mm spacing) either within or surrounding the WE. The laser settings were varied to minimize hole size (1% power) and maximize uniformity (4% speed, 100% frequency), as shown in Fig. 2. Membranes were then patterned with 20 nm Ti / 100 nm Au and 250 nm Ag by Ebeam evaporation (Angstrom Engineering) through a laser cut paper mask in the form of a standard three-electrode system, as previously described [8]. The Ag reference electrode was then converted to Ag/AgCl by treatment with 50 mM $FeCl_3$. The Au WE was CNT-modified by drop casting 2 μL of 1 mg/mL CNT (single-walled CNT powder, Carbon Solutions Inc.) dissolved in 1:1 ethanol and N-methyl-2-pyrrolidone, followed by evaporation of the solvent under a 121°C heat gun. To allow electrical contact with the electrodes patterned on the bottom side of the PETE membrane, 1 mm wide strips of copper tape were attached to the electrode contact pads to bridge from the bottom to the top of the membrane. After assembly, 36-gauge wires were soldered to the copper tape contacts to connect to the potentiostat for electrochemical measurements.

C. Flexible Resistive Heater

The flexible resistive heater was comprised of a 20 nm Cr / 100 nm Au thin-film patterned on a 25.4 μm-thick polyimide film (Kapton, Dupont). Metal coating on the polyimide substrate was achieved by Ebeam evaporation through a laser cut paper mask. The resulting traces (shown in Fig. 1 inset) are 1 mm wide and span a total length of 143 mm, resulting in 50.8 Ω resistance. Strips of copper tape were affixed to the contact pads to connect to a power supply for testing. The temperature of the media was then monitored by inserting a K-type thermocouple into the ECM top chamber.

D. ECM Assembly and Sterilization

PDMS mixed at a 10:1 ratio was used to adhere the modified PETE membranes to the cleaned 3D printed pieces, which were allowed to cure overnight at 37°C. The use of a low temperature prevents significant thermal expansion and glass transition of the MED610, which would cause the membrane to wrinkle upon cooling. Then, the top and bottom chamber were adhered together using the same PDMS curing procedure, along with the resistive heater and 13 mm diameter glass coverslips on the bottom chamber and the lid to allow visualization of the cell culture. Once fully cured, the platform was sterilized with 70% ethanol and dried under UV.

E. Mammalian Gut Epithelial Cell Culture

A tri-culture of three cell lines was grown in the ECM, consisting of a 1:1:1 ratio of Caco-2 enterocytes (ATCC: HTB-37), RIN14B cells, which are a model enterochromaffin cell type that secretes 5-HT (ATCC: CRL-2059), and HT29-MTX goblet cells (Sigma Aldrich: 12040401). Cells were seeded at 15×10^4 cells/well (total) and sustained in Dulbecco's Modified Eagle Medium (DMEM) with 10% Fetal Bovine Serum (FBS) in a 37°C, 5% CO_2 incubator for 8 days. Cells were then fixed and stained for evaluation of the monolayer morphology and 5-HT content. Fixation was achieved by 10 min treatment with 4% paraformaldehyde. Immunocytochemistry (ICC) included: cell permeabilization for 10 min with 0.1% Triton X-100, blocking for 30 min with 1% BSA and 22.5 mg/mL glycine, 1 h incubation with 1:500 diluted goat-α5HT primary antibody at RT, 1 h incubation with 2 μg/mL donkey-αgoat-AlexaFluor594 secondary antibody at RT in the dark, and counter staining with 1 μg/mL DAPI for 1 min. Cells were then imaged using a Zeiss LSM 700 confocal microscope.

F. Fluidic Connection Between Modules

The flow system connected the modules with Tygon E-3603 tubing (Inner diameter: 1/16-inch, Outer diameter: 3/16-inch, Cole-Parmer). A three-way stopcock (T-junction) with luer connections (Cole-Parmer) allowed for dilution of DMEM in crayfish saline. DMEM was fed through the ECM by a Genie Plus syringe pump (Kent Scientific) at 100μL/min. Then, crayfish saline was fed into the T junction between ECM and EPM driven by a FH100 peristaltic pump (Thermo Scientific) at flow rates of 1mL/min or 5mL/min, as stated in

the following procedures. Outflow from the EPM was done by continuous suction, maintaining fluid at a fixed height of ~0.5 cm within the EPM.

G. Electrochemical 5-HT Monitoring

The ECM contains membrane-integrated electrochemical electrodes for detection of redox active species after diffusion from apical to basolateral surfaces. Cyclic voltammetry (CV) was performed to characterize ferrocene dimethanol (FDM) diffusion through the membrane, in which voltage was scanned from 0 – 0.5 V at 300 mV/s to obtain a time resolution of 3.3 s/cycle. Chronoamperometry (CA) was performed as a higher time resolution method to detect instantaneous injection events. CA detection of 10 μL injections of 2 mM FDM or 10 μM 5-HT was done by holding a potential of 0.5 V, which is above the redox potential of both species, producing spikes in response to injection events. All electrochemical procedures were run with a VSP-300 potentiostat (BioLogic).

H. Crayfish Ex Vivo Preparation and Electrophysiology

Adult crayfish (*Procambarus clarkii*), purchased from commercial suppliers, were used for all electrophysiology experiments. Animals were chilled on ice for 15 min before dissection. The abdominal ventral nerve cord was removed from the animal, pinned down in the PDMS-filled EPM using fine insect pins, and bathed in crayfish saline as the baseline medium for electrophysiology experiments.

Electrophysiological procedures followed established protocols [11]. Extracellular electrophysiology experiments involved placement of a silver wire stimulating electrode on the nerves of the last abdominal ganglion (A6) of the nerve cord. Recording electrodes were placed on the connectives between anterior ganglia (A2-A3) for action potential recording. A6 nerves were stimulated to recruit sensory afferents that excite LG action potentials. After the LG threshold was determined, subthreshold stimuli were applied at an interstimulus-interval of 90 s. Baseline recordings were obtained by perfusing crayfish saline through both inlets with the following flow rates: syringe pump – 100 μL/min through the ECM; peristaltic pump – 1 mL/min through T-junction. To determine the effects of 5-HT on LG excitability, 1 mL 1.5 mM 5-HT was injected into the top chamber of the ECM using a syringe with the same flow rate (100 μL/min), resulting in a 10X dilution of 5-HT in the EPM. 5-HT was then washed out by perfusion with crayfish saline.

Intracellular electrophysiology experiments involved placement of a glass microelectrode filled with 2 M potassium acetate and ~25 MΩ resistance into the axon of the LG to measure changes in excitatory postsynaptic potentials (EPSPs) evoked by A6 afferent stimulation. Baseline (crayfish saline only), DMEM diluted with saline at ratios of 1:9, 1:4, 1:1, and pure DMEM were perfused into the dish. Dilutions were prepared in batches and perfused through the peristaltic pump at 5 mL/min. Subthreshold stimuli were applied every 90 s and LG EPSPs were recorded. After baseline recordings, each DMEM dilution was applied for 45 min to allow equilibration of the LG to the stimuli.

III. Results and Discussion

A. Optimizing Laser Cut Parameters to Modify PETE Membranes

Microporous polyester membranes, such as the PETE membranes used here, are widely used in transwell cell cultures because of their hydrophilicity, smooth flat morphology, transparency, and chemical and mechanical stability [12]. These membranes are made from polyethylene terephthalate which has very good chemical resistance [13]. However, this limits the use of wet etching to pattern customized features in these membranes. Therefore, laser cutting was used as a facile, mask-free method to modify a commercial 0.4 μm PETE membrane for the purpose of increasing trans-membrane diffusion. Laser parameters were optimized to minimize the diameter of holes and the number of skipped holes, maximizing uniformity of the pattern. These parameters include the power output of the laser, the speed of the laser head movement across the design pattern, and the frequency of laser pulses per second, which are all graded on a 0 to 100% scale. It was determined that using the lowest power setting (1% power) was necessary to minimize hole diameter, so laser speed and frequency were varied for further optimization (Fig. 2). As shown in Fig. 2a, when laser speed was varied from 1 to 5%, faster speeds resulted in smaller hole diameters. Varying laser frequency, higher frequency resulted in fewer skipped holes. As shown in Fig. 2b, the optimal laser parameters of 1% power, 4% speed, and 100% frequency produced the smallest holes (diameter 119 μm $\pm$ 26 μm) with the best uniformity. Therefore, these parameters were used to modify all PETE membranes.

B. Diffusion Monitoring With Modified PETE Membranes

Electrochemical monitoring of FDM diffusion was performed to investigate the enhanced diffusion capability of PETE membranes modified with laser cut holes either i. within or ii. surrounding the WE (Fig. 3a), compared to Ø. an unmodified membrane. After assembling membranes inside ECM modules, 1 mL 1 mM FDM was injected at the top surface of each membrane and diffusion across the membrane and into the bottom chamber (2 mL bulk volume) was monitored by CV (Fig. 3). No flow was used during these experiments. Both modified membranes increased the maximum signal reached after injection (i. 77%, ii. 55% of 1 mM FDM control), corresponding to higher concentrations of diffused FDM compared to unmodified membranes (Ø. 11%). The modified membranes also showed higher diffusion rates (i. 29.6 μM/s, ii. 91.7 μM/s) when compared to unmodified (Ø. 0.23 μM/s), calculated as maximum current signal divided by time to reach maximum signal. Diffusion rates of the modified membranes were significantly higher than unmodified membranes, up to 450-fold. These results indicate the utility of modifying 0.4 μm PETE membranes with patterns of larger holes for more rapid diffusion needed for real-time dynamic monitoring.

CA is capable of more rapid detection of individual injection events (0.1 s/measurement). This is essential to detect 5-HT release events from cells, which occur on the order of milliseconds [4]. Since this method shows lower molecular

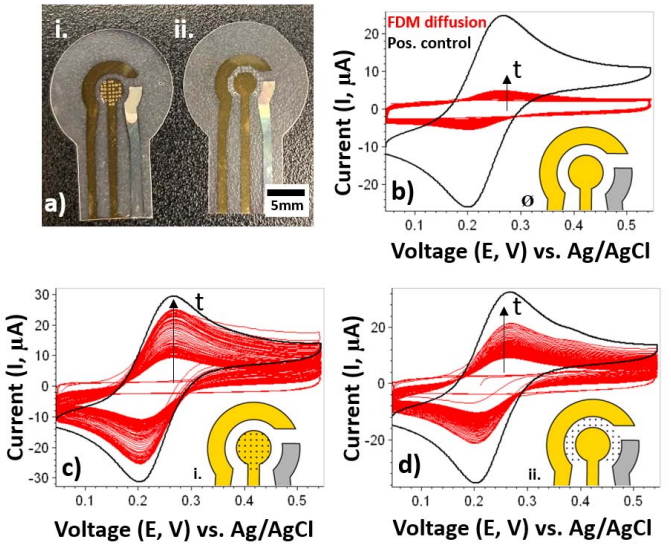

Fig. 3. Laser cut hole-modified PETE membranes (a) show enhanced diffusion via CV detection of injected FDM (b-d). (b) Ø - Unmodified membrane, (c) i.- holes patterned within the WE, and (d) ii. - holes patterned surrounding the WE. Black – 1mM FDM in whole volume (positive control). Red – 1mM FDM injection and diffusion over 200 CV cycles. Scan rate of 300 mV/s, 3.3 s/cycle.

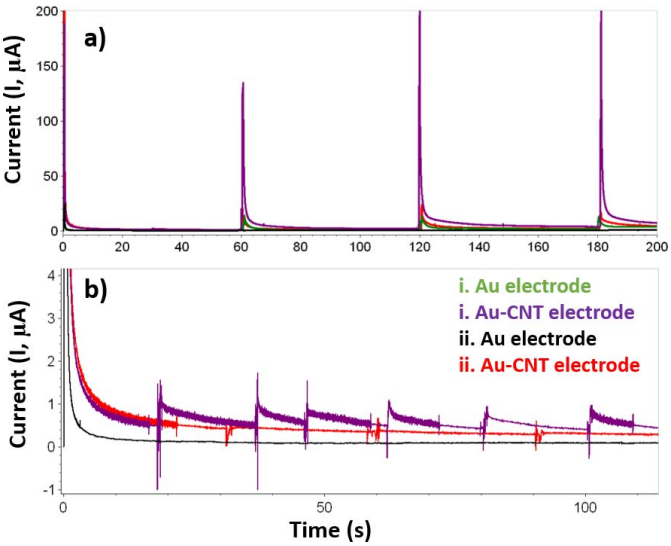

Fig. 4. CA detection of 10 μL injections of (a) 2 mM FDM and (b) 10 μM 5-HT. The legend applies to both graphs.

selectivity and is less quantitative for concentration-specific measurements, it should be performed alongside CV measurements to capture a breadth of information. Electrodes modified with laser cut holes and CNT coatings were tested in Fig. 4 for their CA detection of 10 μL injections of 2 mM FDM and 10 μM 5-HT.

The Cottrell equation states:

$$|i| = \frac{nFAC\sqrt{D}}{\sqrt{\pi t}} \tag{1}$$

where i is the measured current, n is the number of electrons transferred in the redox reaction, F is Faraday's constant, A is electrode surface area, C is species concentration, D is the species diffusion coefficient, and t is time.

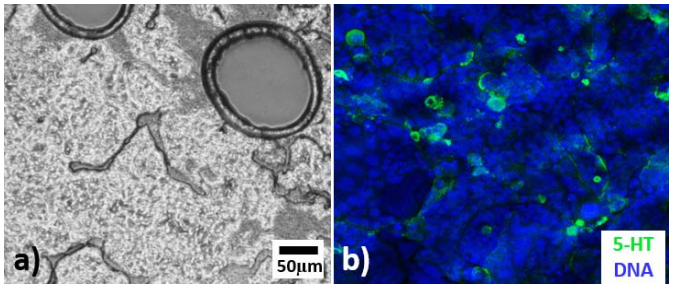

Fig. 5. Gut cell tri-culture within ECM. (a) Brightfield microscopy, +20% contrast. (b) ICC fluorescence microscopy, showing cells stained for 5-HT and nuclei, +20% contrast, +60% brightness. Scale bar applies to (a) & (b).

As confirmed by (1), the peak and time-equilibrated current will increase with increasing concentration of redox species and electrode surface area. Fig. 4a shows that the Au-CNT electrodes have higher current peaks (i. 190 μA, ii. 19 μA) compared to their Au counterparts (i. 13 μA, ii. 0.3 μA), indicating that CNT coating increases electroactive surface area, as corroborated by previous work [9]. Interestingly, laser cut holes within the WE show much higher current responses than holes surrounding the WE (approximately 10x higher). According to (1), this increase could either be due to increased local diffusion at the WE, or because of increased electrode surface area due to increased micro-texture at the hole circumference, which is coated with Au and CNT.

Fig. 4b mimics cell 5-HT release events by apical injections of 10 μM 5-HT, which is within the expected concentration range secreted by the *in vivo* gut epithelium [4]. The Au-CNT electrode with holes within WE was the only electrode to show a significant response, with $\sim$1 μA peaks per injection event. This demonstrates that CNT coating is necessary for 5-HT detection, and patterning holes directly within the WE greatly enhances the possibility of real-time monitoring of 5-HT release from cell cultures.

C. Gut Epithelial Cell Culture Sustained Within the ECM

Fig. 5 shows the growth of healthy gut epithelial monolayers on the modified PETE membranes within the ECM. This membrane is optically transparent, allowing for brightfield imaging (Fig. 5a). ICC staining indicates that, as expected, the monolayer contains approximately a 1/3 proportion of 5-HT containing RIN14B cells (Fig. 5b, green). Both images show that the monolayers form good cell-cell contacts, despite sections that are sub-confluency. Further, it is apparent that cells grow right up to the laser cut holes in the membrane, where any secreted molecules would diffuse readily to the basolateral surface of the membrane for detection.

To evaluate the ability of the flexible resistive heater to achieve and maintain a temperature of 37°C within the ECM, DMEM was incubated in the ECM and a 7.4 V DC voltage was applied across the electrode (Fig. 6a). In this DMEM incubation study, the serpentine resistive heater had a resistance of 50.8Ω which required an input power of 0.9W (0.122 A), which allowed it to ramp up from 19.6°C (RT) to 37.1°C in 27 minutes and plateau at 38.4°C. In the equilibrium state, the heat generated by the resistive heater was equivalent to

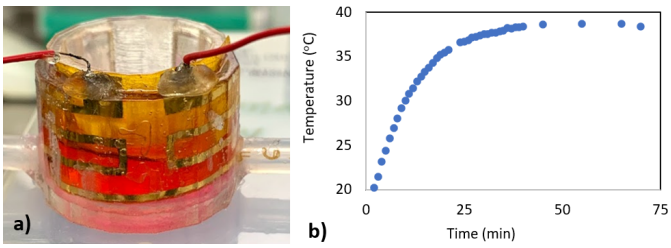

Fig. 6. Flexible heater testing. (a) Image of heater fitted within the ECM bottom chamber. (b) Plot of solution temperature over duration of applied voltage.

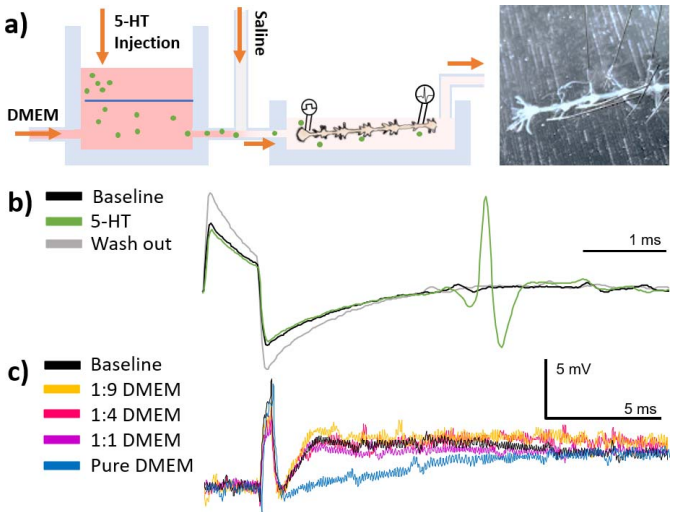

Fig. 7. (a) Left: Cross-sectional schematic of transport through the platform, as pictured in Fig 1, during an electrophysiology experiment. Schematic not drawn to scale. Right: Image of isolated crayfish nerve cord. (b) Extracellular recordings show an action potential in the LG neuron due to injected 5-HT at a subthreshold stimulus (10.2 V), which was washed out with saline indicating a 5-HT-specific response. Scale bar denotes 1 ms in the x direction, no y axis is necessary for action potential measurement. (c) Intracellular recordings of LG EPSPs show effects of different DMEM dilutions compared to baseline (saline only) at a subthreshold stimulus (4 V). Scale bar denotes 5 mV in y direction and 5 ms in x direction.

the heat lost to the environment. The plateaued temperature continued to remain within the target temperature range, which is near body temperature, beyond 60 minutes and is adequate to support cell behavior and viability while applied (Fig. 6b).

D. Neural Responses to 5-HT and DMEM

Fig. 7a illustrates the intended concept of the electrophysiology experiment, in which 5-HT is injected into the top chamber of the ECM, diffuses across the PETE membrane, and is transported through the bottom chamber of the ECM where flow of DMEM transports it through fluidic tubing to the EPM. The DMEM and 5-HT are diluted by crayfish saline through the T-junction and the resulting solution is perfused over the crayfish nerve cord in the EPM.

Here, we show the effects of 5-HT and DMEM separately in Fig. 7b and 7c, respectively. In Fig. 7b, 1 mL 1 mM 5-HT was injected into the ECM top chamber to test 5-HT transport to the EPM and modulation of LG activity. 5 min after injection, traces of LG spike activity indicate that 5-HT was transported to the crayfish nerve cord where it had an excitatory effect, which was reversible upon washout. Fig. 7c shows that DMEM dilutions in crayfish saline (1:9, 1:4, and 1:1 DMEM to saline) had minimal effects on the LG EPSP, which is a measure of subthreshold nerve activity. Pure DMEM, however, caused a major decrease in the initial parts of the EPSP, corresponding to early excitatory inputs. This confirms that DMEM alone modulates neuronal activity, but DMEM dilutions in saline, even as low as a 1:1 ratio, may provide a reasonable baseline for cell-released 5-HT experiments. At this ratio, the dilution factor of 5-HT in the EPM chamber can be minimized to preserve high concentrations of cell-released 5-HT upon perfusion of the nerve cord.

IV. Conclusion

This is the first work to our knowledge building an integrated platform for the combination of *in vitro* mammalian gut cell studies and *ex vivo* crayfish nerve cord electrophysiology studies. The integration of features such as a flexible heater, to avoid the need for bulky incubators, and *in situ* electrochemical sensors patterned on a specialized membrane, which enhances both diffusion and cell culture, shows promising results for use in future GBA research. Indeed, the millisecond timescale signaling dynamics, which underlie gut cell secretion and neuronal activation, require real-time detection capabilities, which was demonstrated here by CA and electrophysiology measurements. Direct fluidic transport and detection of injected 5-HT serves as a proof-of-concept demonstration of the platform, where future work will aim to investigate the effects of luminal stimulants on gut epithelial cell culture molecular release and downstream neural activity.

References

[1] K. N. Browning, S. Verheijden, and G. E. Boeckxstaens, "The Vagus nerve in appetite regulation, mood, and intestinal inflammation," *Gastroenterology*, vol. 152, no. 4, pp. 730–744, Mar. 2017.

[2] M. Carabotti, A. Scirocco, M. A. Maselli, and C. Severi, "The gut-brain axis: Interactions between enteric microbiota, central and enteric nervous systems," *Ann. Gastroenterol., Quart. Publication Hellenic Soc. Gastroenterol.*, vol. 28, no. 2, pp. 203–209, Jan. 2015.

[3] B. Bonaz, T. Bazin, and S. Pellissier, "The vagus nerve at the interface of the microbiota-gut-brain axis," *Frontiers Neurosci.*, vol. 12, p. 49, Feb. 2018.

[4] P. Bertrand, "Real-time detection of serotonin release from enterochromaffin cells of the guinea-pig ileum," *Neurogastroenterol. Motil.*, vol. 16, pp. 514–551, Jul. 2004.

[5] J. M. Yano *et al.*, "Indigenous bacteria from the gut microbiota regulate host serotonin biosynthesis," *Cell*, vol. 161, pp. 264–276, Apr. 2015.

[6] C. Chu *et al.*, "The microbiota regulate neuronal function and fear extinction learning," *Nature*, vol. 574, no. 7779, pp. 543–548, Oct. 2019.

[7] J. Herberholz, *Serotonergic Modulation of Aggression. Serotonin: Biosynthesis, Regulation and Health Implications, F.S. Hall*. Hauppauge, NY, USA, NOVA Science, 2013, pp. 27–51.

[8] D. H. Edwards, W. J. Heitler, and F. B. Krasne, "Fifty years of a command neuron: The neurobiology of escape behavior in the crayfish," *Trends Neurosci.*, vol. 22, no. 4, pp. 153–161, Apr. 1999.

[9] A. A. Chapin, P. R. Rajasekaran, J. Herberholz, W. E. Bentley, and R. Ghodssi, "Dynamic *in vitro* biosensing with flexible microporous multimodal cell-interfacial sensors," in *Proc. 20th Int. Conf. Solid-State Sensors, Actuat. Microsyst. Eurosensors XXXIII (TRANSDUCERS EUROSENSORS XXXIII)*, Berlin, Germany Jun. 2019, pp. 944–947.

[10] C. G. Y. Ngan *et al.*, "Optimising the biocompatibility of 3D printed photopolymer constructs *in vitro* and *in vivo*," *Biomed. Mater.*, vol. 14, no. 3, Mar. 2019, Art. no. 035007.

[11] Y. C. Liu and J. Herberholz, "Sensory activation and receptive field organization of the lateral giant escape neurons in crayfish," *J. Neurophysio.*, vol. 104, no. 2, pp. 674–684, Aug. 2010.

[12] Sterlitech, Kent, WA, USA. *Membrane Disc Filters: Polyester Membrane Filters*. Accessed: Apr. 27, 2020. [Online]. Available: https://www.sterlitech.com/media/wysiwyg/pdfs/Sterlitech_Catalog2016_PETE_.pdf
[13] B. Lepoittevin and P. Roger, "Poly (ethylene terephthalate)," in *Handbook of Engineering and Specialty Thermoplastics*, vol. 3. Hoboken, NJ, USA: Wiley-Scrivener, 2011, ch. 4, pp. 97–126.

Ashley A. Chapin was born in Philadelphia, PA, USA, in 1993. She received the B.S. degree in biological engineering from the Massachusetts Institute of Technology, Cambridge, MA, USA, in 2015. She is currently pursuing the Ph.D. degree in bioengineering with the University of Maryland at College Park, College Park, MD, USA. For eight months in 2016, she worked as a Researcher at the SUNY Downstate Medical Center to continue volunteer research she had started as a high school science project. In 2017, she worked as a Teaching Assistant with the Department of Bioengineering (BIOE), University of Maryland at College Park. Her research interests include the development, design, and fabrication of biosensor and electrochemical sensor systems. She is currently applying these strategies toward biochemical monitoring of *in vitro* cultured tissues. She won the UMD Bioscience Day Best Poster Award in 2019, the IBBR-REFI Travel Award in 2019, and an A. James Clark School of Engineering Finalist position in the 3-MT Competition in 2020.

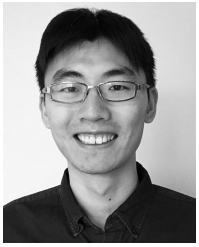

Jinjing Han received the B.S. degree in electrical and computer engineering from Rutgers University, New Brunswick, NJ, USA, in 2017. He is currently pursuing the Ph.D. degree in electrical and computer engineering (ECE) with the University of Maryland at College Park, College Park, MD, USA. From 2017 to 2019, he worked as a Teaching Assistant with the Department of Electrical and Computer Engineering, University of Maryland at College Park. His research interests include the design and development of microdevices for chemical and biological sensing. He received the ECE Outstanding TA Award in 2019.

Ta-Wen Ho received the B.S. degree in life science from National Tsing-Hua University, Hsinchu, Taiwan, in 2016. He is currently pursuing the Ph.D. degree in neuroscience and cognitive science with the University of Maryland at College Park, College Park, MD, USA. During his sophomore year, he joined an exchange program for six months at the School of Life Science and Biotechnology, Shanghai Jiao Tong University, Shanghai, China. He worked in several neuroscience laboratories, working with invertebrates and vertebrates, throughout his undergraduate training. Since 2017, he has been a Teaching Assistant of different neuroscience-related lecture and lab courses with the Department of Psychology (PSYC) and the Department of Biology (BIOL). His research interests include cellular and molecular mechanisms underlying the interplay between prior social experience and alcohol intoxication, using neurophysiology and neuropharmacology approaches.

Jens Herberholz received the bachelor's and master's degrees in zoology from Albert-Ludwigs University, Freiburg, Germany, in 1992 and 1995, respectively, and the Ph.D. degree in natural sciences from Technical University, Munich, Germany, in 1999. From 1999 to 2005, he was a Post-Doctoral Associate and a Research Scientist with Georgia State University and the Center for Behavioral Neuroscience, Atlanta, before becoming a Faculty Member of the Psychology Department, University of Maryland at College Park, in 2005. He served as the Director of the Neuroscience and Cognitive Science Program from 2013 to 2017 and is currently the Co-Director of the Brain and Behavior Initiative (BBI), University of Maryland at College Park. In his work, he uses crayfish as a primary animal model for research, which allows for cellular and circuit-level analysis using neurophysiological, neuroanatomical, neurochemical, and neuroimaging techniques. His current research interests include identifying the structure and function of decision-making neural circuitry and understanding the interconnections between neural activity patterns and motor action. He is an Associate Editor of *Behaviour* journal and a member of the Editorial Board for the journals *Invertebrate Neuroscience* and *Frontiers in Invertebrate Physiology*.

Reza Ghodssi (Fellow, IEEE) is the Herbert Rabin Distinguished Chair in Engineering and the Director of the MEMS Sensors and Actuators Laboratory (MSAL), Department of Electrical and Computer Engineering (ECE) and the Institute for Systems Research (ISR), University of Maryland (UMD) at College Park. He was the Director of the Institute for Systems Research (ISR) from 2009 to 2017. During this time, he launched a number of interdisciplinary initiatives, such as the Maryland Robotics Center (MRC) and the Brain and Behavior Initiative (BBI), aimed at enhancing the impact of ISR research efforts on society while building a more interactive faculty, staff, and student community across different disciplines in the institute. He has obtained eight U.S. patents, with another seven pending. He has over 150 journal publications and 334 refereed conference papers. His research interests include the design and development of micro/nano/bio devices and systems for chemical and biological sensing, small-scale energy conversion, and harvesting with a strong emphasis toward healthcare applications. He is the University of Maryland Distinguished Scholar-Teacher, AVS, and ASME. He is a Co-Editor of the *MEMS Materials and Processes Handbook* (2011). He served as an Associate Editor for the *Journal of Microelectromechanical Systems* (JMEMS) for 12 years. He is an Associate Editor of *Biomedical Microdevices* (BMMD).